RESEARCH ARTICLE

Journal
American Ceramic Society

Evaluation of the sterilization effect on biphasic scaffold based on bioactive glass and polymer honeycomb membrane

Audrey Deraine Coquen[1,2] | **Bartosz Bondzior**[3,4] | **Laeticia Petit**[2] | **Minna Kellomäki**[2] | **Emmanuel Pauthe**[1] | **Michel Boissière**[1] | **Jonathan Massera**[2]

[1]ERRMECe, Equipe de Recherche sur les Relations Matrice Extracellulaire-Cellules (EA1391), Université de Cergy-Pontoise, Maison Internationale de la Recherche (MIR), rue Descartes, Neuville sur Oise Cedex, France

[2]Laboratory of Biomaterials and Tissue Engineering, Faculty of Medicine and Health Technology, Tampere University, Tampere, Finland

[3]Photonics Laboratory, Tampere University, Tampere, Finland

[4]Institute of Low Temperature and Structure Research PAS, Wrocław, Poland

Correspondence
Audrey Deraine Coquen and Jonathan Massera, Bioceramics, Bioglasses and Biocomposites Group, Faculty of Medicine and Health Technology, Tampere University, Korkeakoulunkatu 3, Tampere SM424 33720, Finland.
Email: audrey.deraine@tuni.fi and jonathan.massera@tuni.fi

Abstract

The sterilization is a core preoccupation when it comes to implantable biomaterials. The most common in industry is the gamma sterilization; however, the radiation used in this method can induce modifications in the material properties. This study investigates the impact of such radiations on the physicochemical properties and biological toxicity of a new biomaterial based on a poly-L-co-D,L-lactide polymer honeycomb membrane and bioactive glass (BG), combined, to form an assembly (membrane/BG assembly). The investigated BGs are the S53P4, which is FDA approved and clinically used, and 13-93B20, a BG containing boron promising for bone regeneration. Infrared and photoluminescence measurements revealed that, upon irradiation, defects are created in the BGs molecular matrix. Defects were identified to be mainly non-bridging oxygen hole center and occur in higher proportion in the 13-93B20 making it more sensitive to irradiation compared to the S53P4. However, the irradiation does not significantly impact the structure of the BGs. On the membrane side, the molecular weight is divided by two resulting in a lower shear stress resistance. However, the membrane honeycomb topography does not seem to be impacted by the irradiation. In contact with cells, no toxicity effect was observed, and BGs keep their bioactive properties by releasing ions beneficial to the cell fate and with no influence on apatite precipitation speed. Overall, this study showed that, despite some impact on the physicochemical properties, the irradiation does not induce deleterious effect on the membrane/BG assemblies and is therefore a suitable method for the sterilization of this novel biomaterial.

KEYWORDS
13-93B20, bioactive glass, gamma irradiation, honeycomb membrane, PLDLA, S53P4

1 | INTRODUCTION

In the 1970s, Larry Hench developed the first bioactive glass (BG). Due to its unique composition, it is able to release ions that stimulate the cells present in the bone to produce new bone and bond to it while degrading.[1] Following this discovery, the S53P4 was developed and is now commercialized as BonAlive (BonAlive Biomaterials Ltd.).[2] Since then, multiple BG compositions have been investigated with the goal to improve the angiogenic properties of BG. Houaoui et al.[3] demonstrated that BG 13-93B20, containing boron, is a highly promising BG for bone regeneration, whereas boron, substituted for SiO_2 in the silicate matrix, was found to be efficient in over-expressing angiogenic markers.[4] Recently, we reported on this BG in combination with a honeycomb membrane with the goal to produce a new biphasic material allowing bone regeneration while protecting the bone defect from invasion by fibrotic tissue demonstrating the promising use of this material as an implant.[5]

When it comes to biomaterials intended for implantation, sterilization is a central preoccupation as there are high risks of infection if the implants are not properly sterilized. Indeed, sterilization allows to eliminate microorganisms found on the implantable materials, therefore preventing the infection risk for the patient. The selection of the sterilization technique must be done with great care and must take into account the feasibility but also the fact that it can affect the materials properties and modify its performances.[6]

Some well-known sterilization methods comprise ethylene oxide, steam, dry heat, and radiation methods.[7] Particularly, gamma sterilization has several advantages. Indeed, sterilization through gamma rays is low cost, is performed at room temperature, fast, has a high penetration in materials, and is associated with a low risk of producing toxic residues.[8,9] Those advantages make gamma irradiation one of the most common sterilization methods, notably in the biomedical industry.[10,11] The regulation recommends the use of a dose of gamma rays that will allow to have a sterility assurance level of 10^{-6} meaning that the probability of finding a viable microorganism on an implantable device should be equal or lower than 10^{-6} to ensure that the material is sterile.[12] The usual recommended dose for medical devices to achieve sterility is 25 kGy.[6,11,13] Yet, Gamma irradiation is known to affect polymers, and particularly biodegradable polymers such as poly-L-CO-D,L-lactide (PLDLA) as well as glasses.

When considering the glass, used in this study as a bioactive, osteopromotive substrate, the radiation damages can lead to a displacement of atom(s) in the BG network upon photon/atom collision and/or may induce ionization producing electron-hole pairs.[14] However, the material response to the radiation is complex. The material composition and structure as well as the nature and the dose of the radiation play an important role in the response of the material to radiation treatment.[15] Although large amount of data is available for glasses used in the immobilization of nuclear waste, such studies are not widely performed on compositions like BG. Thus, when investigating a new biomaterial, it is of outmost importance to investigate the effect of the gamma-irradiation on its physicochemical properties and its cytotoxicity when in contact with cells.

As our developed biphasic materials also possess a polymeric membrane, one should keep in mind that not only the radiation may affect the inorganic substrate but also the polymer and the interfacial bonds between the polymer and the BG. The polymeric membrane, deposited on the BG, as shown in Ref. [5], is made of PLDLA. However, it is generally accepted that high dose of gamma radiation leads to a decrease in the average molecular weight (Mw) of the PLDLA through chain scission.[16] Studies have shown that such effect typically occurs at dose greater than 25 kGy. However, already at 25 kGy, simulations have shown that the Mw of PLDLA 96/4 was decreased by almost 50%.[16] In the case of our biphasic material, it is therefore crucial to assess the change in average Mw as well as to ensure that the interface between the BG and the membrane remains stable postirradiation.

In this context, the impact of gamma radiation on the BG structure was investigated using Fourier transform infrared (FTIR), photoluminescence (PL), and UV–vis spectroscopy. The impact of radiation on the polymer membrane was assessed by size exclusion chromatography (SEC) to valuate changes in the average Mw, and scanning electron microscopy images were recorded to ensure that the honeycomb structure was maintained postirradiation. The interface stability, between the BG and the membrane, was assessed by shear stress testing. Finally, cells were cultured at the surface of the radiated biphasic material and their behavior compared to cells cultured on biphasic materials that were not exposed to radiation. This study shine light on the impact of gamma radiation, regularly used for biomaterials sterilization, on the physicochemical properties of biphasic materials as well as on the interfacial interaction between the polymer membrane and the BG substrate.

TABLE 1 Composition of the bioactive glasses (BGs) in mol%.

BG	mol%						
	Na_2O	CaO	P_2O_5	SiO_2	K_2O	MgO	B_2O_3
S53P4	22.66	21.77	1.72	53.85	–	–	–
13-93B20	6.0	22.1	1.7	43.7	7.9	7.7	10.9

2 | MATERIALS AND METHODS

2.1 | Material preparation

S53P4 and 13-93B20 BGs were prepared from analytical grade K_2CO_3 (Alfa Aesar, Thermo Fisher), Na_2CO_3, $NH_4H_2PO_4$, $(CaHPO_4)(2(H_2O))$, $CaCO_3$, MgO, H_3BO_3 (Sigma Aldrich), and Belgian quartz sand. The nominal oxide compositions (in mol%) of the experimental BGs are presented in Table 1.

The 60 g batch of S53P4's raw reagents were placed in the furnace preheated at 600°C and then temperature increased to 1200°C and kept for 1 h and then melted at 1450°C for 3 h. The 60 g batch of 13-93B20's raw reagents were placed in the furnace at RT and heated to 800°C. The temperature was kept for 15 min to decompose the raw materials and then melted at 1450°C for 1 h. Both glasses were melted in a platinum crucible in an electrical furnace, in air. The molten BGs were then casted into a preheated (400°C) graphite mold to obtain a rod with diameter 14 mm. The BGs rods were then annealed overnight at 40°C below the respective glass transition temperature of the BGs overnight and let to cool down to room temperature. After annealing, the rods were cut into 2 mm thick discs and polished with SiC paper (grit 320, 500, 800, 1200, 2400, and 4000, from Struers). All samples were kept in a desiccator until further use.

Prior to the membrane deposition, the polished BGs were immersed in TRIS buffer solution and incubated at 37°C for 24 h. TRIS solution was prepared from Trisma base and Trisma HCl (Sigma Aldrich) at pH 7.40 ± 0.02 at 37 ± 0.2°C. After incubation, the solution was removed, and BGs were allowed to dry under a fume hood over night before membrane deposition. This method is referred to as the conditioning. Conditioning has been shown to improve the membrane/BG interaction.[5]

Honeycomb membranes were fabricated from a solution of PLDLA with an M/M% ratio of 96/04 and surfactant dioleoyl phosphatidylethanolamine (DOPE) at 10 and 0.1 mg/mL respectively, in chloroform. PLDLA purified, medical grade, PURASORB PLD 9620 (inherent viscosity midpoint of 2.0 dL/g), was purchased from Corbion Purac and DOPE from Sigma Aldrich. The honeycomb membranes were produced by the breath figure method as described in Figure S1 and as previously reported in Ref. [17]. Briefly, the polymer solution was deposited drop by

drop onto BG materials (untreated and conditioned), and then the solvent was allowed to evaporate in a humidity chamber at 80% ± 5% RH, under airflow. The membranes were air dried at room temperature and then washed two times with 70% ethanol in order to remove the surfactant. Samples were air-dried again and stored in a desiccator until further use.

Finally, before irradiation, the membrane/BG assemblies were disinfected in two successive EtOH 70% baths and stored in homemade individual plastic pockets and then irradiated at room temperature using a ^{60}Co gamma cell (2000 Ci) as source of gamma radiation having a dose rate under 28 kGy. The gamma irradiation was performed by IONISOS.

2.2 | Characterization

Before measuring the infrared (IR) spectra of the BGs, the membrane was removed by polishing, and they were crushed by hand in a mortar to obtain a powder. The IR spectra were recorded using a Spectrum Two FTIR spectrophotometer Perkin Elmer (PerkinElmer) in attenuated total reflectance mode with a diamond crystal puck, to assess the possible changes induced by the sterilization. All IR spectra were recorded within the range of 400–4000 cm^{-1} with a resolution of 2 cm^{-1} and 64 accumulation scans. All spectra were background corrected and normalized to the band with maximum intensity and presented from 600 cm^{-1} because of the air absorption that makes the signal below 600 cm^{-1} unreliable.

PL spectra were recorded with an FLS-1000 (Edinburgh Instruments) spectrofluorometer equipped with double excitation and emission monochromators and with a 450 W xenon lamp as excitation source. Spectra were recorded from 300 to 920 nm with a slid width of 2 mm, a step of 2 nm, and an excitation wavelength of 266 nm. The measurements were performed on bulk BGs and repeated multiple times and on different days to confirm the trends discussed in Section 3.

The UV–vis absorption spectra of the BGs were measured using a spectrophotometer (UV-3600 Plus) in the 200–1800 nm range with a step of 0.5 nm.

For the SEC, the membranes were dissolved from 12 membrane/BG assemblies in 2 mL of tetrahydrofuran (THF, Fischer scientific) and filtered before measurement in order to analyze the polymer Mw before and after irradiation. A Merck Hitachi 7000 series was used to analyze the samples, equipped with two Waters Styragel columns (HR5E and HR1), an L-7200 autosampler taking 20 μL of the solution to analyze, an L-7100 pump, an L-7350 column oven set at 35°C, and an RI 5450 detector. Solutions were

eluted in THF at 1 mL/min. The Mws were calibrated using polystyrene standards high EasiVial (Agilent).

The shear stress test was performed using two aluminum plates that were clamped to a TA1 texture analyzer (Lloyd materials testing, AMETEK) equipped with a 100 N load cell as in Ref. 5 The specimen to be tested was fixed in-between the plates, by solvent-free double-sided tape (tesa ECO FIXATION). Briefly, shear force on the membrane was created by pulling the upper plate at 1 mm/min, whereas the bottom aluminum plate remained fixed. The test was performed on five-to-six samples. The illustration of the setup can be found in Ref. [18]. The surface of detachment (SOD) was measured using the freehand selection tool from Fiji software to draw the contour of the places where the membrane detached and measure the area selected. The areas obtained for each place were then summed to obtain the total area from which the membrane detached and divided by the number of samples to obtain the average SOD.

2.3 | Material-cell interaction

Prior to cell culture, the nonirradiated samples were disinfected in two successive EtOH bath during 1 and 2 min, respectively, and then allowed to dry for 10 min before use. Between the baths, the samples were allowed to dry during 5 min under the laminar hood.

The irradiated and nonirradiated samples were preimmersed in 1 mL of cell culture medium for 24 h before seeding the cells. Pre-osteoblastic MC3T3 cells (E1 subclone 4, from ATCC, ref: CRL-2593) were cultured in minimum essential medium α (αMEM) Gibco (Thermo Fisher Scientific) supplemented with 10% fetal bovine serum and 1% penicillin/streptomycin, in a humidified atmosphere of 5% CO_2 at 37°C.

Cells were seeded at a density of 20 000 cells/samples, and three samples were used. The morphology of the cells was observed after 24 h, 72 h, and 7 days of culture. At each time point, the cells were fixed with 3% (w/v) paraformaldehyde solution dissolved in PBS (Sigma Aldrich) for 15 min and then permeabilized with 0.1% (v/v) Triton X-100 (Sigma Aldrich) for 10 min. Nonspecific binding sites were blocked by incubating the assembly in PBS containing 1% bovine serum albumin (BSA, Sigma Aldrich) for 1 h. The cytoskeleton and nuclei of the cells were stained, respectively, with 1:50 FITC-labeled phalloidin (Sigma Aldrich P5282) and 1:1000 4′,6-diamidino-2-phenylindole dihydrochloride (Sigma Aldrich D9542) in PBS-BSA 0.5% for 1 h. Each incubation with antibodies was performed in the dark in a humid atmosphere. Samples were then washed in PBS-BSA 0.5%, mounted in Prolon-gold (Invitrogen), and observed under an LSM710 confocal microscope (Carl Zeiss).

During the cell culture, at each time point (preincubation, 24 h, 72 h, and 7 days after cells seeding), 1 mL of culture medium was collected from each sample and diluted in 9 mL of deionized water to quantify the change in ion concentration over time. The preincubation time point is presented before 0 in the curves. Inductively coupled plasma (ICP)-optical emission spectroscopy analysis was conducted with an Agilent 5110 instrument (Agilent technologies) equipped with an SPS 4 autosampler, to quantify the presence of phosphorus (P), sodium (Na), calcium (Ca), silicate (Si) (for both BGs) and boron (B), potassium (K), and magnesium (Mg) (only for 13-93B20) in the medium collected during the cell culture. Wavelength values for the analysis were as follows: P, 213.618 nm; Ca, 317.933 nm; Si, 288.158 nm; B, 249.678 nm; K, 766.491 nm, and Mg, 279.800 nm. The results are presented as cumulative data ± standard deviation (SD).

3 | RESULTS AND DISCUSSION

Before discussing the impact of the gamma irradiation on various membrane/BG assembly properties (including cell-membrane/BG assembly interactions), the structural and luminescent properties of the selected BGs, S53P4 and 13-93B20, are first presented. The IR spectrum of S53P4 BG in Figure 1a exhibits multiple bands that can mainly be related to Si–O bonds. The shoulder at ≈ 660 cm^{-1} and the band at ≈ 750 cm^{-1} can be attributed to bending vibrations of the Si–O^{-} end groupings.[19–21] The main band at ≈ 915 cm^{-1} can be assigned to Si–O^{-} (non-bridging oxygen—NBO) asymmetric stretching vibrations of the [SiO$_4$] units[22,23] followed by the band at ≈ 1010 cm^{-1} which is related to Si–O–Si asymmetric stretching vibration.[22] A faint shoulder can be seen ≈ 1250 cm^{-1} and might be connected to longitudinal asymmetric stretching of Si–O–Si according to Kopani et al.[24] The band at ≈ 1465 cm^{-1} can be associated with carbonate groups presence due to an incomplete decarbonization.[19,20,25] The spectrum of 13-93B20 has similar bands compared to that of the IR spectrum of S53P4 while also having a few differences. The band between 600 and 800 cm^{-1}, with a pick at ≈ 720 cm^{-1}, can be associated with B–O–B bending vibrations.[22] The main bands in the 800–1100 cm^{-1} region can be related to a joint contribution from the previously mentioned band related to Si–O bonds and from B–O bonds in [BO$_4$] units especially at 916 and 1010 cm^{-1}.[22] The shoulders at ≈ 1225 cm^{-1} can be related to BO$_2$O^{-} triangles and at ≈ 1400 and ≈ 1470 cm^{-1} can be associated to BO$_3$ groups and carbonate groups whose signature might be covered

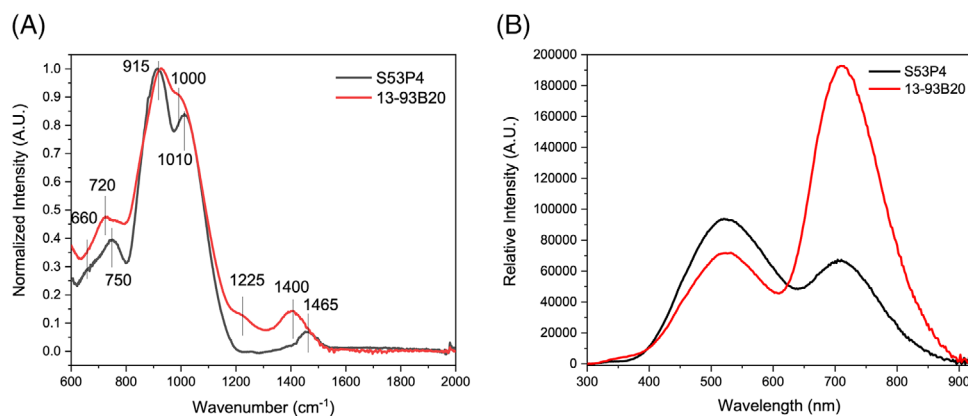**FIGURE 1** Fourier transform infrared (FTIR) (A) and photoluminescence (B) spectra of the bioactive glasses (BGs) as prepared (λ_{exc} = 266 nm).
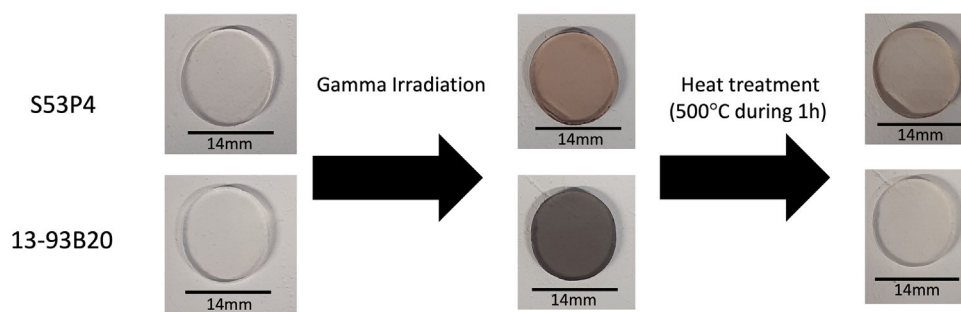

FIGURE 2 Pictures representing pictures of the bioactive glasses (BGs) before and after irradiation and after heat treatment (in that order) showing the reversibility of the color's appearances.

by the BO_3 groups signal.[19,26,27] In summary, although S53P4 spectra mainly depict the presence of SiO_4 units with bridging and NBOs, the structures of 13-93B20 present a joint contribution of the silica network, and mainly BO_3 along with BO_2O^- and BO_4 units that are fully integrated within the BG structure.

The PL spectra, of the 2 investigated BGs, at 266 nm excitation are presented in Figure 1b. They exhibit two emission bands centered at 532 and 710 nm which can be assigned to oxygen deficient centers (ODCs)[28] and NBO hole center ([NBOHC], molecular structure: $\equiv Si\text{–}O^-$),[29,30] respectively. Although a larger amount of ODC is suspected in S53P4 than in 13-93B20, the 13-93B20 possesses a larger amount of NBOHC probably due to the presence of various borate units.[31,32]

3.1 | Effect of the gamma irradiation on the BG

The investigated BGs were irradiated using gamma radiations with a dose of 26–29 kGy. After irradiation, the

BGs became dark, S53P4 being less dark (Figure 2). The darker color of the BGs visible after radiation treatment is a clear sign of defect formation as demonstrated by Rautiyal et al.[14]

As in Rautiyal et al., the formation of defects is evidenced from the changes in the UV–vis absorption spectra after radiation treatment.[14] As depicted in Figure 3a,b, the absorption coefficient in the 300–1000 nm range increases after irradiation, the increase being larger in the absorption spectrum of 13-93B20 BG (Figure 3c).

The shoulder at 450–550 nm can be assigned to defects like ODC,[14,33] and the shoulder at 550–650 nm can be attributed to defects like NBOHC and/or peroxy radicals (molecular structure: $\equiv Si\text{–}O\text{–}O^-$).[14,33] E^- centers, known to have an absorption band in the range of 600–730 nm, are also expected to form during the radiation treatment.[34] The absorption bands centered at 440 and 620 nm can be related to H_I and H_{II} defect centers, defined as trapped holes on one or two NOBs on the same SiO_4 tetrahedron,[35] respectively. Similar defects were reported in silicate glasses by El-Kheshen.[36] According to Griscom et al., ODC, peroxy linkage, and/or E′ centers (molecular structure: Si^-) with an absorption band at 300–350 nm are
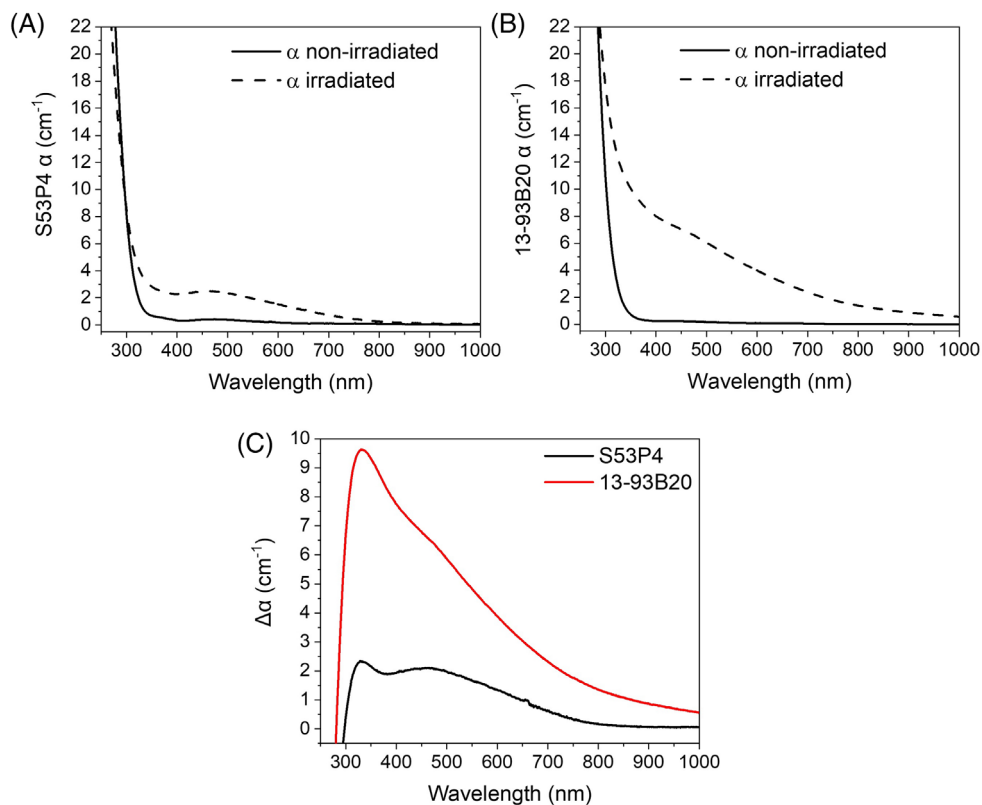
FIGURE 3 UV–vis absorption spectra represented by the absorption coefficient of S53P4 (a) and 13-93B20 (b) as prepared or after irradiation, and spectra of the difference in absorbance coefficient (α) between irradiated and nonirradiated samples (c) ($\Delta\alpha = \alpha$ [irradiated]—α [nonirradiated]).

also expected.[33] In the 13-93B20 BG, the increase in intensity of the absorption bands at 350–450 nm could be related to boron bound oxygen hole centers (BOHC, $\equiv$B–O–Si$\equiv$) according to Möncke et al.[37] BOHC's or hole trapped centers with an absorption band between 500 and 600 nm are also suspected to form.[31] As depicted in Figure 3c, a larger amount of defects are expected to be formed during the radiation treatment in the 13-93B20 indicating that this BG is more sensitive to gamma irradiation than S53P4, probably due to the presence of BO_3 and BO_4 units. Griscom et al.[38] described a core-silicate-clad-borosilicate prototype fiber that shows a higher radiation sensitivity in the cladding material compared to the core. They stated that this higher sensitivity of the borosilicate cladding material is due to the defects formed upon irradiation and particularly the "boron E′ centers." Those centers are planar BO_3 units that, upon irradiation, trap an electron and are therefore charged (-1), whereas the Si E′ centers are not charged, which make the boron E′ centers less stable than their Si counterpart. This might be what happens in our BG and can explain the higher radiation sensitivity of the 13-93B20. This is in agreement with the darker coloration of the 13-93B20 after irradiation as shown in Figure 2.

One should point out that the formation of defects has no noticeable impact on the structure of the BGs (Figure S2) although an increase in bridging oxygen (BO) at the expense of NBO was reported after radiation treatment in Refs. [39, 40]. However, the doses used in these studies were orders of magnitude higher than the dose used in our study. The radiation treatment has an impact on the spectroscopic properties but only for 13-93B20 as seen in Figure 4: The PL emission bands between 300 and 900 nm decreases after irradiating 13-93B20 revealing a decrease in the number of ODC and NBOHC in this glass in agreement with Refs. [39, 40]. 13-93B20 seems to be more sensitive to the irradiation than S53P4 most probably due the presence of BO_3, BO_2O^-, and BO_4 units and of a large amount of NBO in its network.

Nevertheless, the identification of the defects presented here requires more investigation with other methods than FTIR and PL such as Raman spectroscopy or electron paramagnetic resonance spectroscopy to provide more information and precisely determine the nature of each defect.

To assess the reversibility of the color change postirradiation, the irradiated samples were reheated at 500°C for 1 h
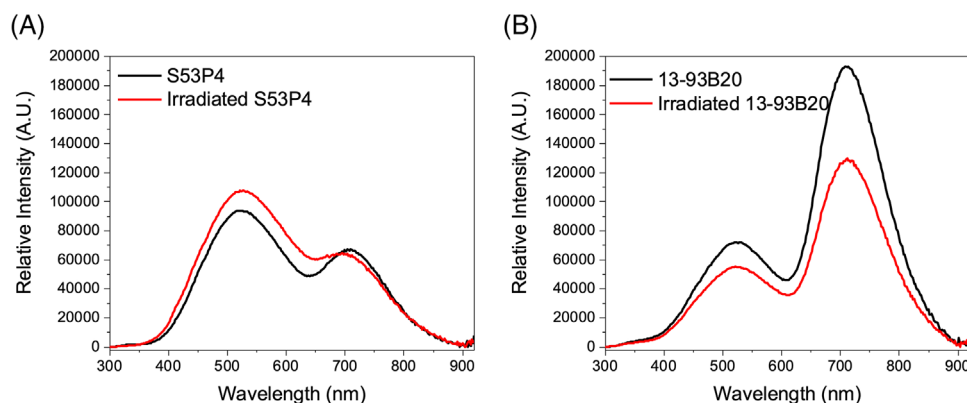
FIGURE 4 Photoluminescence spectra of S53P4 (a) and 13-93B20 (b) before (black curve) and after (red curve) irradiation.
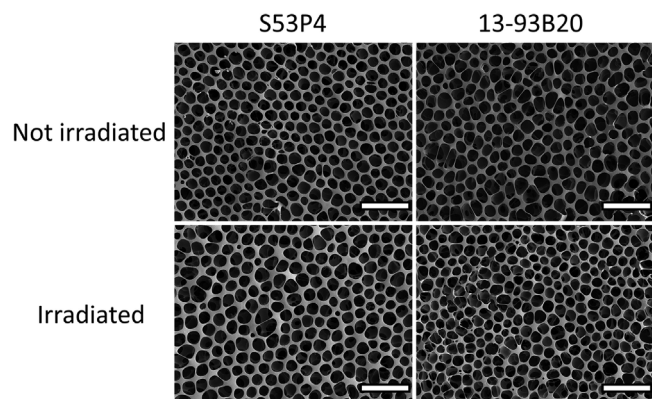

FIGURE 5 Scanning electron microscopy (SEM) images of the membranes deposited on the S53P4 and 13-93B20 substrates both before and after irradiation (scale bar 20 μm).

(Figure 2). This temperature was chosen because it is lower than the T_g of the BGs and would allow relaxation without damaging the BG structure. In Figure 2, it can be seen that all samples recovered a color similar to their original one. This suggests that reversible structural changes are occurring during the irradiation of the samples. This reversibility of the color of the BGs induced by irradiation has already been described by Procházka et al.[41] and El-Kheshen.[36]

3.2 | Effect of the gamma irradiation on the membrane/BG assembly

As shown in Figure 5, the polymer retains the honeycomb structure after irradiation. However, the Mw of the polymer decreases from ≈350.000 to ≈175.000 g/mol after irradiation, independently of the BG composition. A similar decrease in Mw of polymer was reported by Nugroho et al.[42] and Shim et al.[16] and can be related to random chain scission. Furthermore, FTIR spectra were recorded pre- and postirradiation, and no significant difference
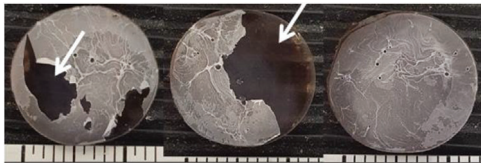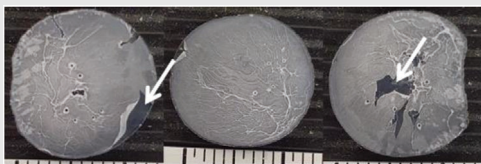
could be evidenced (data not shown). This agrees with a study by Shim et al.[16] who reported that, at gamma-rays doses ranging from 25 to 500 kGy, no significant difference in the polymer chain, and notably the polymer functional groups, before and after irradiation could be seen. In addition, Pérez Davila et al. reported a 99.8% similarity in FTIR spectra recorded pre- and postirradiation (25 kGy) of PLA 3D scaffolds.

Photographies of the membrane/BG assemblies after the shear stress test and SOD are shown in Table 2. Prior to irradiation, the SOD comprises between 2 and 10 mm^2. When comparing the SOD of the nonirradiated S53P4 and 13-93B20 membrane/BG assemblies, we can see a larger surface area detached on the S53P4 than from the 13-93B20 (9.79 vs. 2.61 mm^2), indicating that the membranes are better attached on the 13-93B20 than on the S53P4 due to the thicker apatite layer and its structure at the surface of the BG as explained in Ref. [5]. One should point out the attachment inhomogeneity of the membrane based on the photographies and the large SD for the shear stress load. After irradiation, the SOD increases while using a lower load indicating a lower attachment of the membrane to the BG. Therefore, it is plausible to think that the radiation treatment leads to a decrease of the membrane attachment points and therefore the membrane resistance to shear stress.

3.3 | Effect of the gamma irradiation on the membrane/BG assembly-cell interaction

MC3T3-E1 osteogenic progenitor cells were seeded on top of nonirradiated and gamma irradiated membrane/BG assembly. In order to estimate, and to discriminate, the potential and resulting effects of the irradiation onto the cell behavior, as controls, nonirradiated membrane/BG assembly samples were simply disinfected prior

TABLE 2 Photographies illustrating membrane/bioactive glass (BG) assemblies before and after irradiation, after the shear stress test.

Samples			Average maximum load (N)	Average SOD (mm^2)
S53P4	Before irradiation		42.60 ± 9.45	9.79 ± 10.89
	After irradiation		33.79 ± 13.05	30.40 ± 23.85
13-93B20	Before irradiation		49.17 ± 19.66	2.61 ± 3.27
	After irradiation		36.69 ± 7.26	10.97 ± 6.64

Note: Pointed by the white arrows, membrane total surface ≈ 154 mm^2.
Abbreviation: SOD, surface of detachment.

FIGURE 6 Confocal images of MC3T3 cells cultured on the membrane part of the materials nonirradiated (disinfected) or irradiated after 24 h and 7 days, scale bars 50 μm. Gray scale images show the honeycomb membrane with a shadow of the cells on it. Magenta = actin filaments, yellow = nucleus.
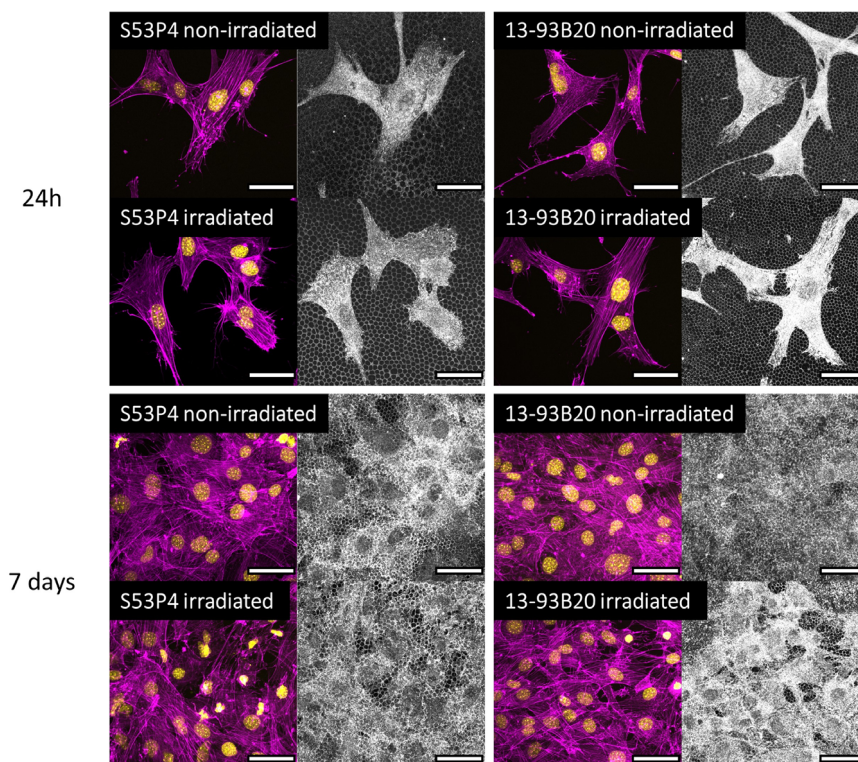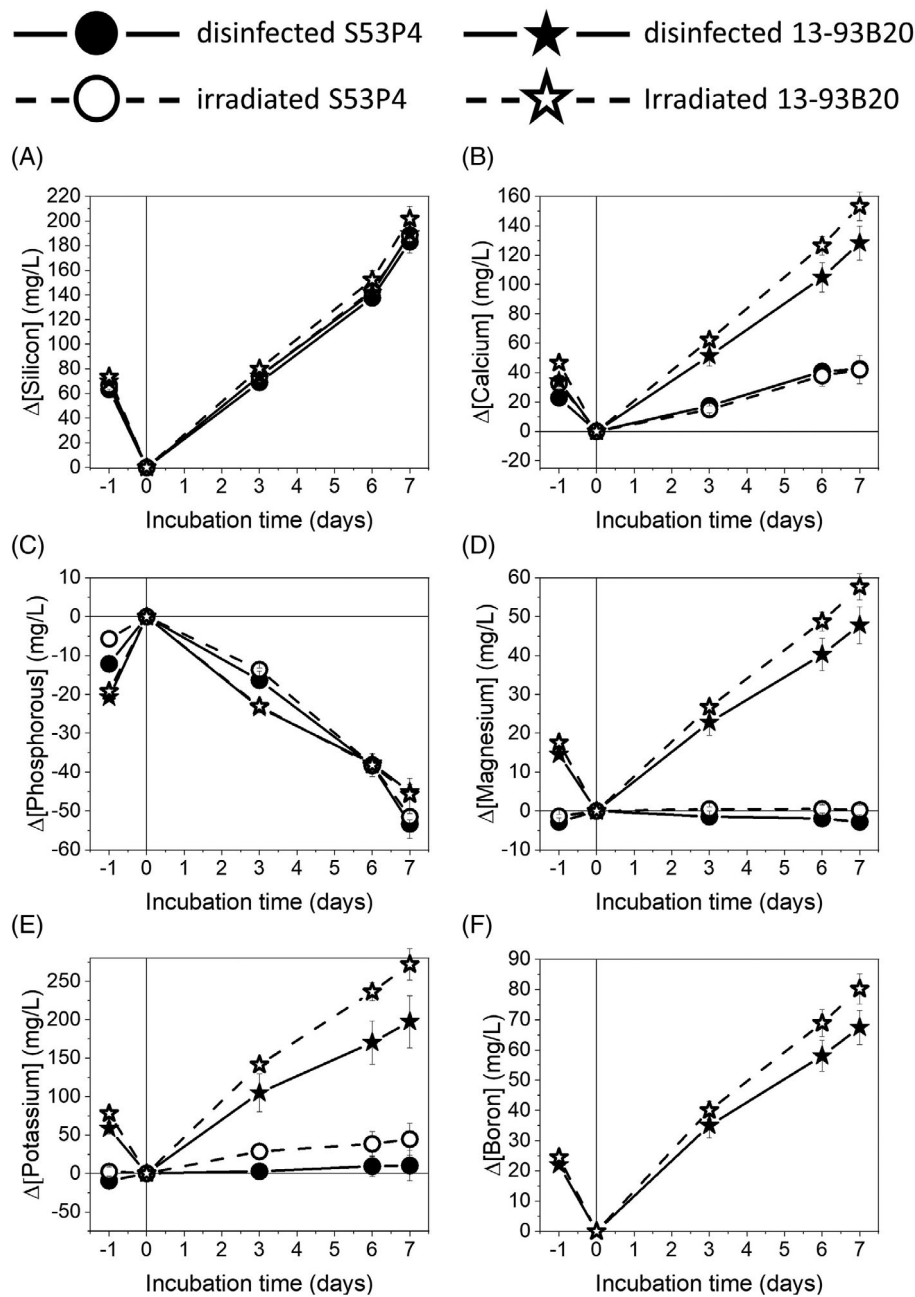
FIGURE 7 Ions release profile of silicon (a), calcium (b), phosphorous (c), magnesium (d), potassium (e), and boron (f) during cell culture up to 7 days of S53P4 nonirradiated (●) or irradiated (○) and 13-93B20 nonirradiated (★) or irradiated (☆). −1 represent the ion release during the preincubation of the materials in complete culture medium and 0 the starting point of the cell testing. Data are presented as cumulative over time.

to cell culture. Cells were cultured on the honeycomb membrane side up to 7 days and had their nucleuses and actin filaments stained and subsequently imaged through confocal microscopy to observe their morphology (Figure 6). Furthermore, the medium during the cell culture was collected and analyzed through ICP to quantify the ion release from the BGs during the experiment (Figure 7).

After 24 h, cells have adhered at the membrane surface and have spread independently of the BG composition and treatment. Actin filaments are visible and organized. Nuclei are well defined and large, showing that the cells grew at the surface of the irradiated membrane/BG assembly similarly than those on the disinfected samples. Furthermore, the honeycomb membrane, visible under the cells (gray scale images), seems to be intact,

independently of the BG composition. After 7 days, cells are confluent. Actin filament organization is well visible like nuclei. The membrane is less visible underneath the cells because of the high number of cells. These results indicate that the gamma irradiation of the membrane/BG assembly does not seem to induce deleterious or cytotoxic effect on the cells.

To confirm this finding, the medium was analyzed through ICP in order to quantify the inorganic ions released by the BGs in the medium during the experiment. The results are presented in Figure 7.

Looking at the ion release from the S53P4, for each considered ion, the release profile is similar irrespective of the treatment. This result indicates that, the defects, resulting from the gamma radiation, do not impact the dissolution rate of the S53P4 BG.

The silicon (Si) release profile of the 13-93B20 is similar to the release profile of S53P4, and no significant variation is observed between the nonirradiated and the irradiated samples. Considering the boron (B) release, we can observe a significant increase in its release when the BG is irradiated. The same pattern can be observed regarding the release profile of calcium (Ca), magnesium (Mg), and potassium (K). As said above, irradiation creates defects in the BGs, and the 13-93B20, due to the presence of borate units like BO_3 and BO_4, is more sensitive to the radiations meaning that more defects are created in this BG. This phenomenon makes the 13-93B20 slightly more soluble when irradiated resulting in a higher release in the medium of Ca, Mg, and K.

Considering the phosphorous (P) concentration, the decrease observed indicates that there is a precipitation of apatite occurring regardless of the BG.[3,20] It is worth noting that, contrary to P, Ca concentration does not decrease. This suggests that Ca ions saturate the solution, whereas P can easily be consumed to form apatite structure at the surface of the membrane/BGs assemblies. Furthermore, there is no significant difference between the irradiated and the nonirradiated samples, making clear that the irradiation does not influence the precipitation speed.

Those results, in combination with the observation from the cell culture, confirm that, even though the irradiation induces the creation of defects in the BG molecular matrix that leads to some modifications in the ion release and the Mws of the polymer membrane that decreases these modifications do not seem harming for the cells. Nevertheless, such observations are not sufficient to ensure that the membrane/BGs assemblies do not have a cytotoxic effect on the cells. Further experiments such as MTT and LDH assays are planned for a future study in order to further analyze the effect of the membrane/BG assemblies and the sterilization on the cells.

4 | CONCLUSION

In this study, the effect of gamma irradiation on scaffolds based on a honeycomb membrane and BG S53P4 and 13-93B20 was investigated.

The gamma irradiation induced the formation of defects such as NBOs and ODCs in the BG molecular matrix. Those defects appear mainly in the silicate and borate network of the BGs. However, it was demonstrated that this effect is reversible upon heat treatment. Furthermore, although the irradiation does not affect the honeycomb membrane topography, it does shorten the polymer chains length by chain scission. The polymer undergoes chain scission, and the membrane has a lower resistance to shear stress compared to the nonirradiated samples. In addition, the irradiation induces modifications in the ion release profile of the BG but does not impact the apatite precipitation speed and does not induce deleterious effect on cells cultured in contact with the membrane/BG assemblies.

Overall, despite the physicochemical modifications of the membrane/BG assemblies, those changes are negligible on the properties of the assemblies. Indeed, the membrane/BG assembly still possesses the features we intended: a honeycomb membrane, strongly attached to its substrate and a BG that maintains its bioactivity without toxic effect on the cells.

ORCID
Bartosz Bondzior https://orcid.org/0000-0002-1764-2427

REFERENCES
1. Jones JR. Bioactive glass as synthetic bone grafts and scaffolds for tissue engineering. In: Jones JR, Clare AG, editors. Bioglasses [Internet]. Chichester, UK: John Wiley & Sons, Ltd; 2012 [cited 2020 Feb 21]. p. 177–201. Available from: http://doi.wiley.com/10.1002/9781118346457.ch12
2. Hulsen DJ, van Gestel NA, Geurts JAP, Arts JJ. S53P4 bioactive glass. In: Management of periprosthetic joint infections (PJIs) [Internet]. Elsevier; 2017 [cited 2019 May 28]. p. 69–80. Available from: https://linkinghub.elsevier.com/retrieve/pii/B9780081002056000045

3. Houaoui A, Lyyra I, Agniel R, Pauthe E, Massera J, Boissière M. Dissolution, bioactivity and osteogenic properties of composites based on polymer and silicate or borosilicate bioactive glass. Mater Sci Eng C. 2020;107:110340.

4. Ojansivu M, Mishra A, Vanhatupa S, Juntunen M, Larionova A, Massera J, et al. The effect of S53P4-based borosilicate glasses and glass dissolution products on the osteogenic commitment of human adipose stem cells. PLoS One. 2018;13(8): e0202740.

5. Deraine A, Rebelo Calejo MT, Agniel R, Kellomäki M, Pauthe E, Boissière M, et al. Polymer-based honeycomb films on bioactive glass: toward a biphasic material for bone tissue engineering applications. ACS Appl Mater Interfaces. 2021;13(25):29984–95. Available from: acsami.1c03759

6. Hasirci V, Hasirci N. Sterilization of biomaterials. In: Fundamentals of biomaterials [Internet]. New York, NY: Springer New York; 2018 [cited 2022 Nov 9]. p. 187–98. Available from: http://link.springer.com/10.1007/978-1-4939-8856-3_13

7. Tipnis NP, Burgess DJ. Sterilization of implantable polymer-based medical devices: a review. Int J Pharm. 2018;544(2):455–60.

8. Dai Z, Ronholm J, Tian Y, Sethi B, Cao X. Sterilization techniques for biodegradable scaffolds in tissue engineering applications. J Tissue Eng. 2016;7:2041731416648810.

9. Jain S, Yassin MA, Fuoco T, Mohamed-Ahmed S, Vindenes H, Mustafa K, et al. Understanding of how the properties of medical grade lactide based copolymer scaffolds influence adipose tissue regeneration: sterilization and a systematic in vitro assessment. Mater Sci Eng C. 2021;124:112020.

10. Jablonská E, Horkavcová D, Rohanová D, Brauer DS. A review of *in vitro* cell culture testing methods for bioactive glasses and other biomaterials for hard tissue regeneration. J Mater Chem B. 2020;8(48):10941–53.

11. Pérez Davila S, González Rodríguez L, Chiussi S, Serra J, González P. How to sterilize polylactic acid based medical devices? Polymers. 2021;13(13):2115.

12. Venugopal B, Chandran S, Ajit A. ISO 11137: an overview on radiation for sterilization of medical devices and healthcare products. In: Timiri Shanmugam PS, Thangaraju P, Palani N, Sampath T, editors. Medical device guidelines and regulations handbook [Internet]. Cham: Springer International Publishing; 2022 [cited 2023 Jan 24]. p. 121–43. Available from: https://link.springer.com/10.1007/978-3-030-91855-2_8

13. Simmons A. Future trends for the sterilisation of biomaterials and medical devices. In: Sterilisation of biomaterials and medical devices [Internet]. Elsevier; 2012 [cited 2023 Jan 24]. p. 310–20. Available from: https://linkinghub.elsevier.com/retrieve/pii/B9781845699321500118

14. Rautiyal P, Gupta G, Edge R, Leay L, Daubney A, Patel MK, et al. Gamma irradiation-induced defects in borosilicate glasses for high-level radioactive waste immobilisation. J Nucl Mater. 2021;544:152702.

15. Jiang N, Silcox J. Electron irradiation induced phase decomposition in alkaline earth multi-component oxide glass. J Appl Phys. 2002;92(5):2310–16.

16. Shim HE, Yeon YH, Lim DH, Nam YR, Park JH, Lee NH, et al. Preliminary study on the simulation of a radiation damage analysis of biodegradable polymers. Materials. 2021;14(22):6777.

17. Calejo MT, Ilmarinen T, Skottman H, Kellomäki M. Breath figures in tissue engineering and drug delivery: state-of-the-art and future perspectives. Acta Biomater. 2018;66:44–66.

18. Lin MR, Ritter JE, Rosenfeld L, Lardner TJ. Measuring the interfacial shear strength of thin polymer coatings on glass. J Mater Res. 1990;5(5):1110–17.

19. Ferraris S, Nommeots-Nomm A, Spriano S, Vernè E, Massera J. Surface reactivity and silanization ability of borosilicate and Mg-Sr-based bioactive glasses. Appl Surf Sci. 2019;475:43–55.

20. Massera J, Hupa L. Influence of SrO substitution for CaO on the properties of bioactive glass S53P4. J Mater Sci: Mater Med. 2014;25(3):657–68.

21. Ouis M, Abdelghany A, Elbatal H. Corrosion mechanism and bioactivity of borate glasses analogue to Hench's bioglass. PAC. 2012;6(3):141–49.

22. Prasad SS, Datta S, Adarsh T, Diwan P, Annapurna K, Kundu B, et al. Effect of boron oxide addition on structural, thermal, in vitro bioactivity and antibacterial properties of bioactive glasses in the base S53P4 composition. J Non-Cryst Solids. 2018;498:204–15.

23. Massera J, Hupa L, Hupa M. Influence of the partial substitution of CaO with MgO on the thermal properties and in vitro reactivity of the bioactive glass S53P4. J Non-Cryst Solids. 2012;358(18–19):2701–7.

24. Kopani M, Jergel M, Kobayashi H, Takahashi M, Brunner R, Mikula M, et al. On determination of properties of ultrathin and very thin silicon oxide layers by FTIR and X-ray reflectivity. MRS Online Proc Libr. 2008;1066:10660703.

25. Koutsopoulos S. Synthesis and characterization of hydroxyapatite crystals: a review study on the analytical methods. J Biomed Mater Res. 2002;62(4):600–612.

26. Kamitsos EI, Patsis AP, Karakassides MA, Chryssikos GD. Infrared reflectance spectra of lithium borate glasses. J Non-Cryst Solids. 1990;126(1–2):52–67.

27. Tainio JM, Salazar DAA, Nommeots-Nomm A, Roiland C, Bureau B, Neuville DR, et al. Structure and in vitro dissolution of Mg and Sr containing borosilicate bioactive glasses for bone tissue engineering. J Non-Cryst Solids. 2020;533:119893.

28. Fournier J, Néauport J, Grua P, Jubera V, Fargin E, Talaga D, et al. Luminescence study of defects in silica glasses under near-UV excitation. Phys Procedia. 2010;8:39–43.

29. Nishikawa H, Shiroyama T, Nakamura R, Ohki Y, Nagasawa K, Hama Y. Photoluminescence from defect centers in high-purity silica glasses observed under 7.9-eV excitation. Phys Rev B. 1992;45(2):586–91.

30. Munekuni S, Yamanaka T, Shimogaichi Y, Tohmon R, Ohki Y, Nagasawa K, et al. Various types of nonbridging oxygen hole center in high-purity silica glass. J Appl Phys. 1990;68(3):1212–17.

31. Fayad AM, Abd-Allah WM, Moustafa FA. Effect of gamma irradiation on structural and optical investigations of borosilicate glass doped yttrium oxide. Silicon. 2018;10(3):799–809.

32. Schuhladen K, Wang X, Hupa L, Boccaccini AR. Dissolution of borate and borosilicate bioactive glasses and the influence of ion (Zn, Cu) doping in different solutions. J Non-Cryst Solids. 2018;502:22–34.

33. Griscom DL. Optical properties and structure of defects in silica glass. J Ceram Soc Jpn. 1991;99(1154):923–42.

34. Mackey JH, Smith HL, Halperin A. Optical studies in x-irradiated high purity sodium silicate glasses. J Phys Chem Solids. 1966;27(11–12):1759–72.

35. Griscom DL. E.S.R. studies of radiation damage and structure in oxide glasses not containing transition group ions: a contemporary overview with illustrations from the alkali borate system. J Non-Cryst Solids. 1974;13(2):251–85.

36. El-Kheshen AA. Glass as radiation sensor. In: Current topics in ionizing radiation research. Vol. 26. London: IntechOpen; 2012. p. 579–602.

37. Möncke D, Ehrt D. Irradiation induced defects in glasses resulting in the photoionization of polyvalent dopants. Opt Mater. 2004;25(4):425–37.

38. Griscom DL, Sigel GH, Ginther RJ. Defect centers in a pure-silica-core borosilicate-clad optical fiber: ESR studies. J Appl Phys. 1976;47(3):960–67.

39. Mao J, Yang K, Chen X, Zhu S, Zhang G, Yang F, et al. Structural changes on the surfaces of borosilicate glasses induced by gamma-ray irradiation. J Am Ceram Soc. 2022;105(8):5178–89.

40. Ollier N, Boizot B, Reynard B, Ghaleb D, Petite G. Analysis of molecular oxygen formation in irradiated glasses: a Raman depth profile study. J Nucl Mater. 2005;340(2–3):209–13.

41. Procházka R, Ettler V, Goliáš V, Klementová M, Mihaljevič M, Šebek O, et al. A comparison of natural and experimental long-term corrosion of uranium-colored glass. J Non-Cryst Solids. 2009;355(43–44):2134–42.

42. Nugroho P, Mitomo H, Yoshii F, Kume T. Degradation of poly(l-lactic acid) by γ-irradiation. Polym Degrad Stab. 2001;7(2):337–43

SUPPORTING INFORMATION

Additional supporting information can be found online in the Supporting Information section at the end of this article.

How to cite this article: Coquen AD, Bondzior B, Petit L, Kellomäki M, Pauthe E, Boissière M, et al. Evaluation of the sterilization effect on biphasic scaffold based on bioactive glass and polymer honeycomb membrane. J Am Ceram Soc. 2024;107:154–165. https://doi.org/10.1111/jace.19406